Tribology International 175 (2022) 107834

Contents lists available at ScienceDirect

Tribology International

journal homepage: www.elsevier.com/locate/triboint

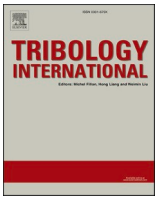

The high temperature tribological behavior of an iron oxide strengthened iron compound obtained from an industrial byproduct

C.H. Ortiz [a,*], A. Esguerra-Arce [b], Johanna Esguerra-Arce [b], A. Bermúdez Castañeda [c], J.C. Caicedo [a], Y. Aguilar [a]

[a] TPMR, Universidad del Valle, Calle 13 No. 100-00, Cali, Colombia
[b] CIMSER, Escuela Colombiana de Ingeniería Julio Garavito, AK. 45 No. 205-59, Bogotá, Colombia
[c] DSIM, Escuela Colombiana de Ingeniería Julio Garavito, AK. 45 No. 205-59, Bogotá, Colombia

ARTICLE INFO

Keywords:
Recycling
High temperature
Wear
Friction coefficient

ABSTRACT

This new material is based on an oxide dispersion strengthened iron, obtained by a partial chemical reduction of ground mill scale for subsequent compaction and sintering. *The mechanical properties* depend on the porosity level and the quantity of the iron oxide reinforcement. Having into account the characteristics of the reinforcement, the tribological behavior was evaluated at two types or ironox compounds under dry sliding conditions. The effect of porosity was evaluated and a comparison with an AISI 1040 steel was done. Experimental test was carried out using a pin on disk tribometer at different temperature. It was found that, on the contrary of AISI 1040 steel, the wear rate of ironox compounds with temperature tends to slow down.

1. Introduction

1.1. Circular economy perspective and byproducts recycling

The worldwide transition from a lineal economy perspective to a circular economy, and its impact on national and international politics, lead to the industry and academia to think about different strategies to add value to industrial wastes. Therefore, in Colombia some regulations and laws have been enacted to define the National Politics for the integral Management of Solid Wastes, such as: the 12th Sustainable Development Goal [1,2] and the CONPES 3874 [3]. As a consequence, since 2019, Gerdau-Diaco, an international steel maker company based in Colombia, and two research groups from the academy worked together in the development of a new material from mill scale, which is an important byproduct generated in this kind of factories. The novel material, called ironox, is a cermet composed of particles of iron oxide (a mix of wüstite and magnetite) and a matrix of iron. This material is produced by partial chemical reduction of mill scale powders, followed by pressing and sintering. The iron oxide particles act as reinforcing and provide a ferrimagnetic behavior to iron [4].

1.2. Oxide dispersion strengthened materials

Oxide dispersion strengthened material are an important type of material used in extreme conditions at high temperatures. Besides improving mechanical properties at high temperatures, the addition of the oxide second particles to a metallic matrix reduces its density. That is the case of Y_2O_3, Al_2O_3 and ThO_2 when are added to Ni composites [5]. Or the case of Al_2O_3 added Mo, which added Al_2O_3 particles increase hardness and compressive strength at high temperatures [6]. Ferritic steels also achieve good mechanical properties with the addition of oxides particles as Y_2O_3 and Al_2O_3. However, the manufacture techniques of this kind of materials are expensive and complicated to achieve at industrial scale [7]. Used techniques for the fabrication of oxide dispersion strengthened materials are via chemical processes, as sol-gel, co-precipitation, hydrothermal, and freeze-drying methods [1]. Meanwhile ironox, the material studied in this research, is obtained by a simple method of chemical reduction, which is easily scalable to industrial scale [4,8].

It is expected that mechanical properties do not diminish so much at high temperatures because two facts: First the iron oxide particles in ironox are not obtained by precipitation from the iron matrix, and secondly, it exists in more quantity than the reinforcing phase of a steel, which is the case of dispersoid composites in comparison to dispersed

* Corresponding author.
E-mail address: christian.ortiz.ortiz@correounivalle.edu.co (C.H. Ortiz).

https://doi.org/10.1016/j.triboint.2022.107834
Received 16 March 2022; Received in revised form 18 July 2022; Accepted 28 July 2022
Available online 3 August 2022

hardened alloys. Fig. 1 shows a scheme of how tensile strength of a $CuAl_2$ dispersed hardened aluminum alloy varies with temperature in comparison to SAP (sintered aluminum powder + Al_2O_3 particles). Although SAP composite is not as strength as the dispersed alloy at low temperatures, the mechanical property does not diminish as much as in the case of the alloy at high temperatures [9].

The solid-state chemical reduction process is the most commonly used method for producing iron powder. The resulting particles are irregular, sponge-like and soft, and are used for processing by powder metallurgical techniques. When processed, these powder particles obtained samples with good strength. In this sense, the powder particles obtained by direct reduction are irregular, but the pressing and sintering process use irregular powders. However, powder metallurgy is a convenient manufacturing process for circular economy due to its advantages, so the metal-ceramic material named "Ironox", has an iron oxide phase with 53 % by weight, and this iron oxide phase is composed of hematite (4.6 %), magnetite (29.6 %) and wüstite (65.9 %), and a metallic phase, which contains 47 % by weight. Furthermore, from the particle size distribution, the resulting particles present an average diameter of approximately 31.9 μm and a specific surface area of 0.507 m2/g. Considering the above, the value of 53 % by weight of the iron phase was chosen as it is closest to the 51 % of the pearlitic phase of the commercial steel AISI 1040. Finally, the maximum hardness of ironox is achieved for 53 % weight of iron oxide particles as reinforcement, and it increases as long as the compaction pressure is higher. A hardness of 78 HRB has been obtained when ironox is manufactured under a compaction pressure of 1405 MPa and a sintering temperature of 900 °C. Moreover, if ironox is compared to an AISI 1040 steel, which contains 51 % weight of pearlite as a reinforcement microconstituent and exhibits a hardness value rounded 95 HRB, it seems that the mechanical properties of ironox do not diminish as much as in the case of steel at high temperatures, even though is not as hard as the AISI 1040.

1.3. High temperature tribology of steel at dry conditions

Low alloy steels are commonly used for machinery parts because of their good mechanical properties, in which tribological conditions influencing the *friction coefficient* and wear rate are very important. At the moment, it is clear that these properties of the system depend on a lot of variables, as normal load, sliding velocity, surface roughness and hardness of the parts, type of material, temperature, among other [10]. Therefore, having into account that the difference in hardness between the counterparts, as well as roughness and microstructure, have a decisive influence on the tribological behavior. Thus, the *friction coefficient* and wear rate have presented several studies showing the effect of these properties on the tribological behavior under dry conditions.

In the case of steels, plastic deformation plays an important role in tribological behavior, involving the formation of a gradient structure,

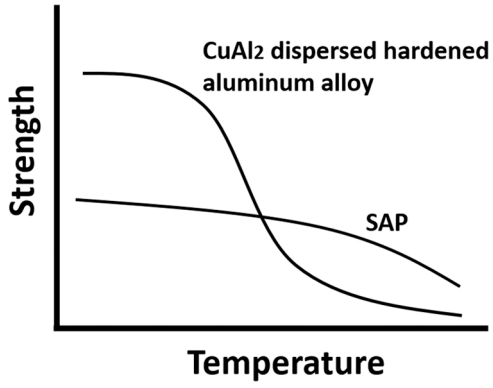

Fig. 1. Scheme of strength variation of a hardened dispersed alloy an a hardened dispersoid composite as a function of temperature.

which consists of a sequence of layer with different levels of deformation and, in consequence, of hardening. Wear of the surface is directly related to the thickness and hardness of that structure, which is fragmented. Therefore, the process is cyclic, involving deformation, strain accumulation and fracture [11]. As was mentioned by Fleming and Suh, there is a crack propagation below the surface, which is increased with the *friction coefficient* [12]. Therefore, wear debris are formed after plastic deformation, hardening and fragmentation inside the layer, and the mechanism of formation of the particles depends on the character plastic delamination wear mechanism, which, in summary, consist of four steps: plastic deformation and hardening of the surface, crack nucleation of the surface, crack propagation, and creation of wear debris.

Besides this wear mechanisms, abrasion and adhesion are also observed in steel at dry conditions. When a soft counterpart is used, as other steel, abrasion and adhesion wear mechanisms are attributed to the fragmentation of the softer material, which produce debris, as was explained for the delamination wear mechanisms [13]. In adhesion, fragmented part is adhered in other parts of the track, or in the counterpart. In abrasion, wear debris caused groves of wear and more release of wear particles. However, the use of a hard ceramic counterpart pin with a steel can generate abrasion wear producing a groove for the action of the pin counterpart [14].

When oxidation occurs, at ambient or high temperature, two scenarios can be found: wear particles can be oxidized and generated more wear, or a protective film can be formed on the track, exhibiting a protective role, diminishing the wear. Therefore, the nature of the oxide film greatly influences the kind of the contact during sliding. Moreover, when those films are penetrated, *friction coefficient* usually increases [15].

The importance of reutilization of waste materials and tribological performance of composite materials is based on being able to obtain new processes and novel materials that provides new applications that respond to current industrial demands, therefore taking into account previous works which have shown the technological path than must be followed. So, in this sense in the literature has been found that the utilization on industrial and agricultural waste materials for the development of metal-matrix composites (MMCs), providing, through the details analysis of an ample varied references source-from the oldest to the newest ones- an insight into the challenges and opportunities for the exploitation to their full potential. Also, it was found that the Al-15 wt. % Mg_2Si composites obtained by in situ casting and characterized in wear test, present high tribo-mechanical properties. Thus, other Al-composites materials have shown considerable improvement in AMC hardness and wear resistance by adding 1.5 % G(wt.) and 10 h of milling, showing homogeneous distribution of the reinforcement particles in the Al-base metal-matrix composite. On the other hand, many reports for diverse composite materials have reported relevant results such as the experimental results that show a distribution of Ce-TZP/Al_2O_3 nanocomposite into the metal matrix is homogeneous and that at 450 °C the hardness and wear resistance improved considerably. Formation of an oxide layer is a manifestation than in nanocomposites produced at 450 °C, worn surface were smoother and the total depth of deformations were not severe. Finally, a novel method for manufacturing new generation of AMCs by addition of 10Ce-TZP (tetragonal zirconia polycrystal)/Al_2O_3 nanoparticles to aluminum via powder metallurgy is devised. Aqueous combustion synthesis is used for dispersoid product and milling-compaction-sintering for AMC fabrication. Then these novel reports have been continued by works where it is presented, the quantitative effect of the following parameter on the one single step pressureless infiltration characteristics of bilayer SiCp/rice-husk ash (RHA) porous performs by aluminum alloys was investigated [16–20].

1.4. Objective of this research

Therefore, the main objective of this article was to evaluated the tribological behavior at high temperatures of two types or ironox

compounds under dry sliding conditions. These types of composites (ironox) present a great contribution to circular economy, since these composites are obtained from products derived from steel transformation processes. In addition, these composites showed excellent wear resistance at high temperatures mainly due to iron oxides, which provide thermal and mechanical stability, as well as act as lubricants. First one has a porous structure while the second one is denser structure. AISI 1040 steel was used as a blank to compare the response of ironox composites, since it is a readily available and low cost steel. In addition, several studies have determined, that this steel is lightweight and has high mechanical properties and good resistance in high friction applications, which is used to manufacture axle, gears, bolts, shaft, among other parts needs in the automotive industry [21]. Experimental test was carried out in a tribometer, using a WC pin as counterpart. Temperatures imposed during the test were: room temperature, 100 °C and 200 °C and, the tribological test were carried out with the purpose of evaluating the wear resistance of composite steels (ironox), where the tribological performance of conventional steels is affected [22]. Finally, the wear track was analyzed by SEM and 2D, 3D perfilometry.

2. Materials and experimental methodology

Cylindrical shaped samples of 12.7 mm diameter and 6 mm height of ironox with 53 % weight of iron oxide particles were synthesized with compaction pressure varying between 1264 and 1405 Mpa. Later, sintering was done at 900 °C in argon atmosphere for 2 h. Samples of same dimensions of AISI 1040 steel were also cut. Used nomenclature in this study was as follows: Ironox compacted at 1264 MPa like: Ironox-P (porous), Ironox compacted at 1405 Mpa like Ironox-D (dense) and AISI 1040 steel like AISI 1040. For the Metallographic analysis, the samples were prepared superficially with an abrasive paper (SiC) following the order of 80, 100, 240, 320, 400, 600, 800, 1000 y 1200 μm consecutively. Subsequently, the surface were polished by means of a metallographic polisher using an alumina solution with a particle size of 0.3 μm, maintaining the same preparation conditions, to later perform a chemical attack, with the purpose of revealing its microstructure by means of an optical microscope, and Rockwell B hardness was measured using a Gnehm Harteprufer digital durometer. Porosity of ironox compounds were achieved with a surface analysis using the IQMaterils software.

For the surface study (roughness), the samples AISI 1040 steel and ironox were prepared superficially with an abrasive paper (SiC) following the order of 80, 100, 240, 320, 400, 600, 800, 1000 y 1200 μm consecutively. After, the roughness was measured using a KLA Tencor D-120 3D perfilometer, making 20 profiles on its with a distance of 0.1 μm between each profile and Apex software was used to calculate specific values. Tribological characterization was performed using a pin on disk Microtest Tribometer MT 4001–98 using a WC sphere of 6 mm of diameter as counterpart with a load of 15 N and with a total distance of 200 m, according to ASTM G99–95a standard [23]. Wear track were analyzed using a JSM 6490LV JEOL SEM to analysis the wear mechanism. Wear rate was determined using a KLA Tencor D-120 3D perfilometer, in order to extract the cross-sectional area of the crack. Each track was mapped 20 times. Wear rate (K) was calculated as the sectional area value divided by the force (F) and sliding distance (S), as express in Eq. 1. The chemical composition was characterized using a JEOL Model JSM 6490LV equipped with an electron dispersive energy X-ray analysis system (EDX), therefore a high-purity Ge EDX detector for the reliable acquisition of EDX spectra was used in this analysis. Therefore, EDX elemental concentration were obtained using the ZAF correction method, because certain factors related to the sample composition, called matrix effects associated with (atomic number (Z), absorption (A), and fluorescence (F)), can affect the X-ray spectrum produced during the analysis of electron microprobe and therefore these effects should be corrected to ensure the development of a careful analysis. The correction factors for a standard specimen of know composition were determined initially by the ZAF routine. The relative intensity of the peak K was determined by dead time correction and a referent correction for the X-ray measured. So, before each quantitative analysis of an EDX spectrum a manual background correction and an automated ZAF correction were carried out.

$$K = \frac{v}{(FxS)} \tag{1}$$

3. Results

3.1. Metallography images and hardness measurements

Fig. 2 show the samples microstructure. Pearlite and ferrite matrix is observed in AISI 1040 steel microstructure, while iron oxide particle dispersed in iron matrix are observed in ironox samples. Porous are also observed in ironox sample, as expected for the manufacturing process of compacting and sintering. Hardness values are show in Table 1.

3.2. Tribological analysis

3.2.1. Wear rate as a function of temperature

Friction coefficient curves at room temperature are show in Fig. 3. At the beginning of the test, a rapid increase of the *friction coefficient* value respect to the distance is observed. In stage I know as running-in *friction coefficient* value for AISI 1040 steel and ironox-D were above 0.44 ± 0.01, while for ironox-P was around 0.47 ± 0.01. This increase in the value of *friction coefficient* corresponds to the interaction between the counterpart (WC) and the initial roughness of the sample; when sliding start at the beginning of the tribological test, the surface material is deformed and removed. Debris particles are formed and remain in the wear track, while some material is ploughed to the track borders [24,25]. This interaction is faster for ironox- P compared to the AISI 1040 steel and ironox-D samples, as shown on the right part of Fig. 3. This can be attributed to the lower hardness of the ironox-P (Table 1), which favors a rapid material detachment [26].

Even, after the running period a steady state is expected, due to the evolution of the contact, this stability is not achieved by any sample up to 200 m, as observed in Fig. 3. On the contrary, *friction coefficient* increases with the distance, it may correspond to the rolling, abrasion and deformation of debris particles on the wear track which promotes material detachment, as long as those particles are hardened. Around 200 m, *friction coefficient* values for every material are 0.38 ± 0.05 for AISI 1040 steel, 0.41 ± 0.05 for ironox-D and 0.51 ± 0.05 for ironox-P. Considering that our tribological pair (ironox surface and WC counterpart), have a high difference in hardness, it was possible to establish a rapid settling stage, for the tribological test at variable temperatures (100 °C and 200 °C).

Friction coefficient curves of samples at 100 °C and 200 °C, are show in Figs. 4 and 5, respectively. *Friction coefficient* increments are evident respect to room temperature behavior. Furthermore, at high temperature a steady state seems to be reached.

For test carried out at 100 °C (Fig. 4), the AISI 1040 steel shows an initial increment in *friction coefficient* values, up to 0.60 ± 0.01, which is related to the initial running-in state. Compared to same test at room temperature, it can be observed: Firstly, the initial stage is shorter at higher temperature, and it is followed by a decrease in the *friction coefficient* until the steady state around 0.49 ± 0.01. Under same conditions, ironox-D also exhibits the initial running stage, which was maintained during longer time respect to room temperature or compared to AISI 1040 steel at 100 °C, and *friction coefficient* values registered were around 0.60 ± 0.01. Later, as in the case of the steel, *friction coefficient* decreased until rich the steady stage, where *friction coefficient* was 0.56 ± 0.01. A very different behavior was observed from ironox-P, because at the initial running-in stage a rapid increment was not observed, as in the other two materials. Indeed, the friction

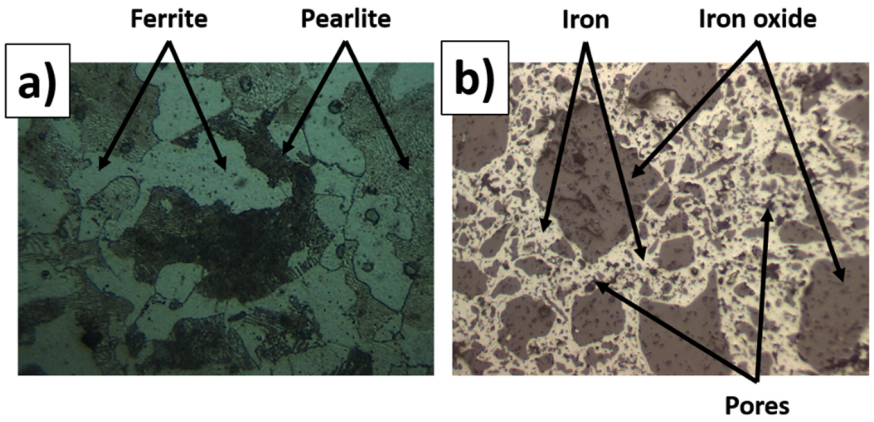

Fig. 2. Microstructural analysis for (a) AISI 1040 steel and (b) Ironox compounds by optical microscopy.

Table 1
Hardness values of the samples.

Sample	Hardness (HRB)
AISI 1040	90 ± 3
Ironox-P	65 ± 8
Ironox-D	69 ± 4

coefficient evolution shows a continuous increasing until the steady stage was reached around at 0.60 ± 0.01.

At 200 °C *(Fig. 5) the* AISI 1040 steel also exhibits the initial running stage, with the same length than at 100 °C, reaching a *friction coefficient* of 0.65 ± 0.01. Later, *friction coefficient* diminishes and increases again to rich the steady stage with a *friction coefficient* of 0.65 ± 0.01. Ironox-D also had a running stage, but it was maintained during a longer distance compared to the test at 100 °C, *friction coefficient* values were around 0.77 ± 0.03. Subsequently, a steady stage was reached around *friction coefficient* values of 0.73 ± 0.01. Similar to test under 100 °C, ironox-P does not exhibit a clear running stage. *Friction coefficient* increased since the beginning until the steady stage, reaching a value of 0.80 ± 0.01.

In general, if *friction coefficient* values are compared ironox-P exhibits higher *friction coefficient* values than ironox-D, which in turn showed higher *friction coefficient* values than AISI 1040 steel. Those results correspond to lower wear rates and lower roughness, as well as the higher hardness presented by the AISI 1040 steel. Although, it is well known that the behavior of the friction coefficient cannot be attributed solely to properties such as hardness, but this behavior is attributed to other factors such as surface properties (roughness) and the influence of the surface stage plays an important role under tribological conditions. In addition, an increase in *friction coefficient* values in all cases when the temperature also increased. This could be attributed to a smoothing effect of the surface because of the temperature, which influenced the evolution of the contact and could change the wear mechanisms presented in the Fig. 6a. Furthermore, by means of Eq. 1, it was possible to calculate the wear rate for all samples as a function of the temperature used during the tribological test. These results showed the same trend that had been presented in the tribological study, where ironox-D presented a lower wear rate compared to ironox-P for all temperature (Fig. 6b). This behavior is attributed to the surface properties (lower roughness) and higher hardness, which generates a decrease in surface wear.

3.2.2. *Wear analysis*

Fig. 7 shows the SEM micrographs from the wear surface for AISI 1040 steel, Ironox-P and Ironox-D as function of applied temperature.

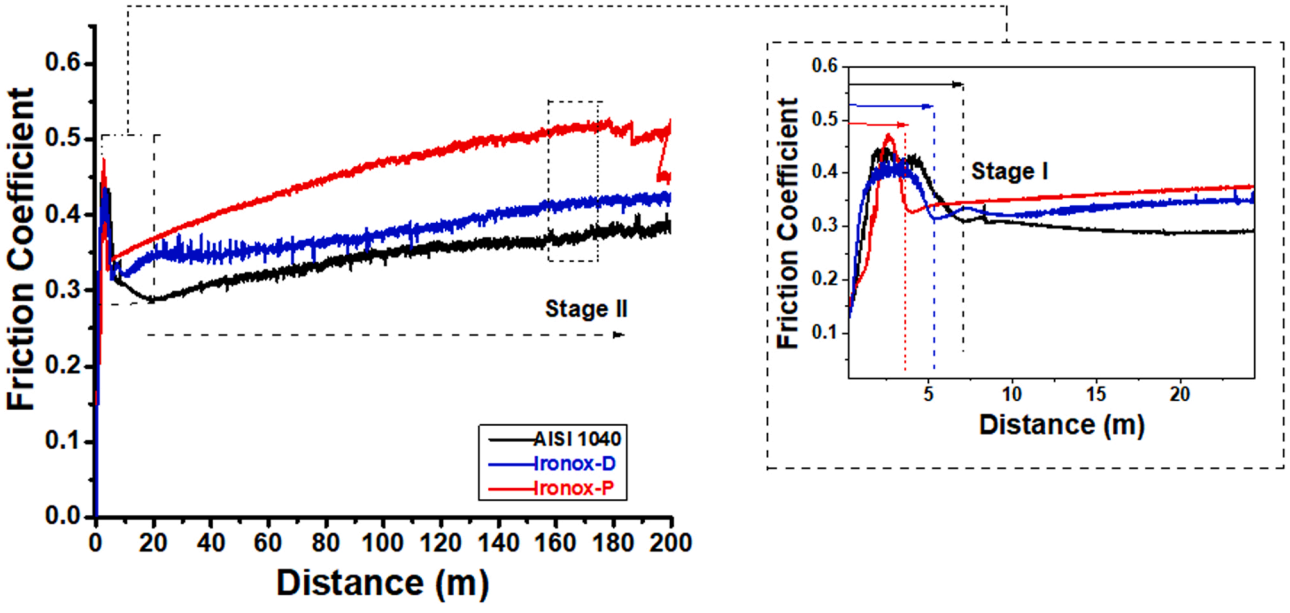

Fig. 3. *Friction coefficient* curves for the samples at room temperature.

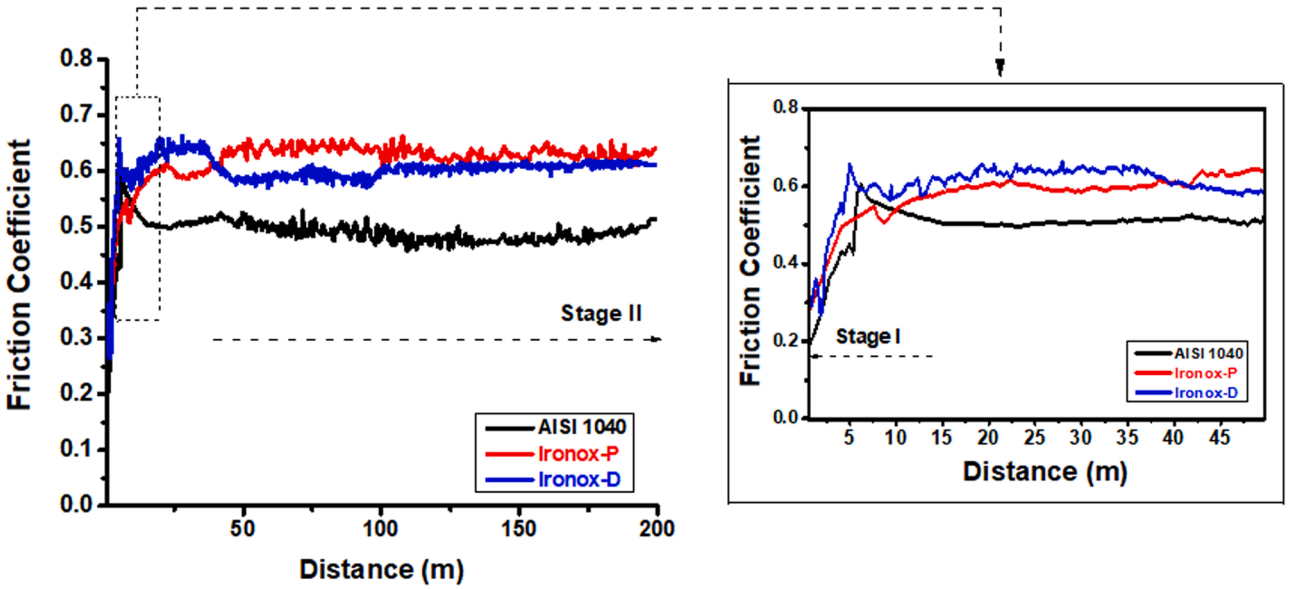

Fig. 4.. *Friction coefficient* for AISI 1040 steel, Ironox-P and Ironox-D as a function of temperature of 100 °C.

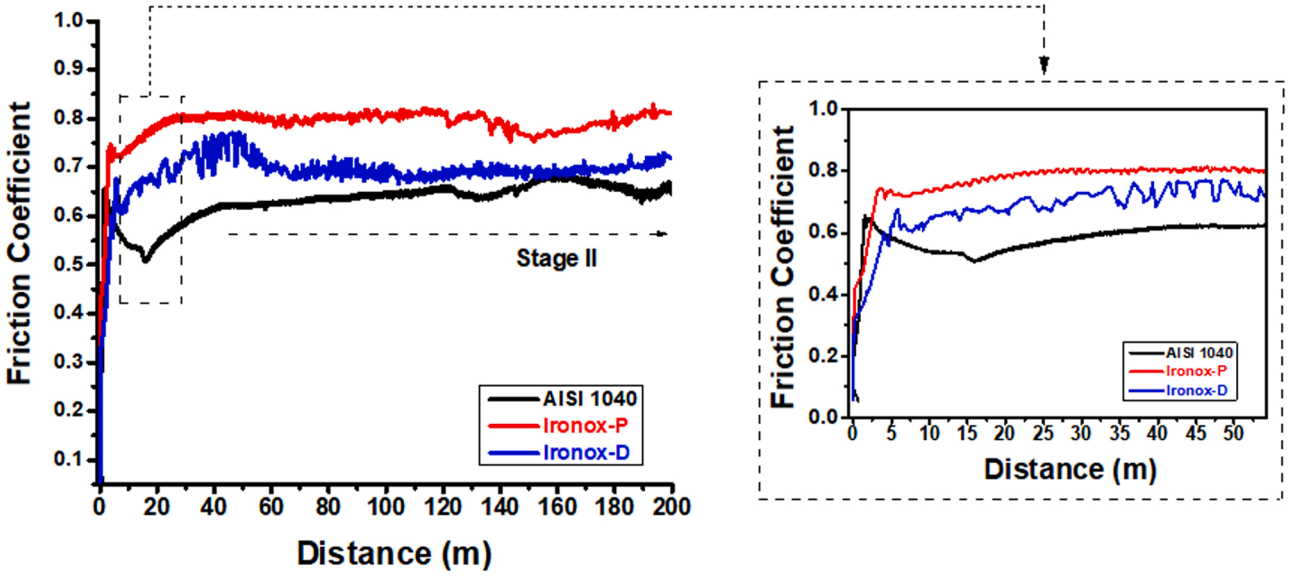

Fig. 5. *Friction coefficient* for AISI 1040 steel, Ironox-P and Ironox-D as a function of temperature of 200 °C.

The Fig. 7a shows the wear track (with a track width of 230 μm) under room temperature, so the wear track is oxidized and contains WC from counterpart according to the EDS analysis, indicating transfer of material from the WC counterpart to the sample (AISI 1040 steel). Moreover, the magnification shows the wear track due to the rubbing, material was removed from the surface of the sample. These particles adhered and spread on the surface when the counterpart (WC) passes over material again. This adhered material can be in turn removed and detached between cycles by deformation or adhesion to the counterpart. Fig. 7a shows the wear track of ironox-P which width was 350 μm. As in the case of steel, the wear track is oxidized and contains WC from the counterpart according to the EDS analysis. Obviously, this track is wider than the track of the steel. Again, adhesion is observed, as well as detachment. In the Fig. 7a a thicker layer seems to be formed respect to what it is observed for ironox-D, its track had a width of 260 μm. Similar to the other material surface, the wear track is oxidized and contains WC from the counterpart according to the EDS analysis. Additionally, the layer formed on the top of the surface seems to be less uniform and narrower compared to images from ironox-P. This could correspond to the higher hardness which leads to a lower wear. Then, the material was not distributed to sideways, even though it could be accumulated below the contact, according to 3D profiles.

Fig. 7b shows the SEM micrographs of AISI steel surface wear at 100 °C. Similar to the test done at room temperature, adhesion is observed, as well as microchipping of the oxidized adhered layer. Furthermore, large number of particles (wear debris) are observed in the track compared to room temperature. This can be attributed to a higher oxidation of the surface. According to chemical analysis by EDS, particles correspond to oxidized steel and, in less proportion, WC debris. This change in composition can produce more brittle material in the surface. Indeed, this material can be ejected to the sideways, which corresponds to a wider wear track of 250 μm, compared to the one obtained at room temperature. Oxidation of the unworn surface is also observed, caused by the high temperature. Fig. 7b show the wear track of ironox-P at 100 °C. Adhesion and oxidation is again observed, as in the test carried out at room temperature. Material detachment from the surfaces are not

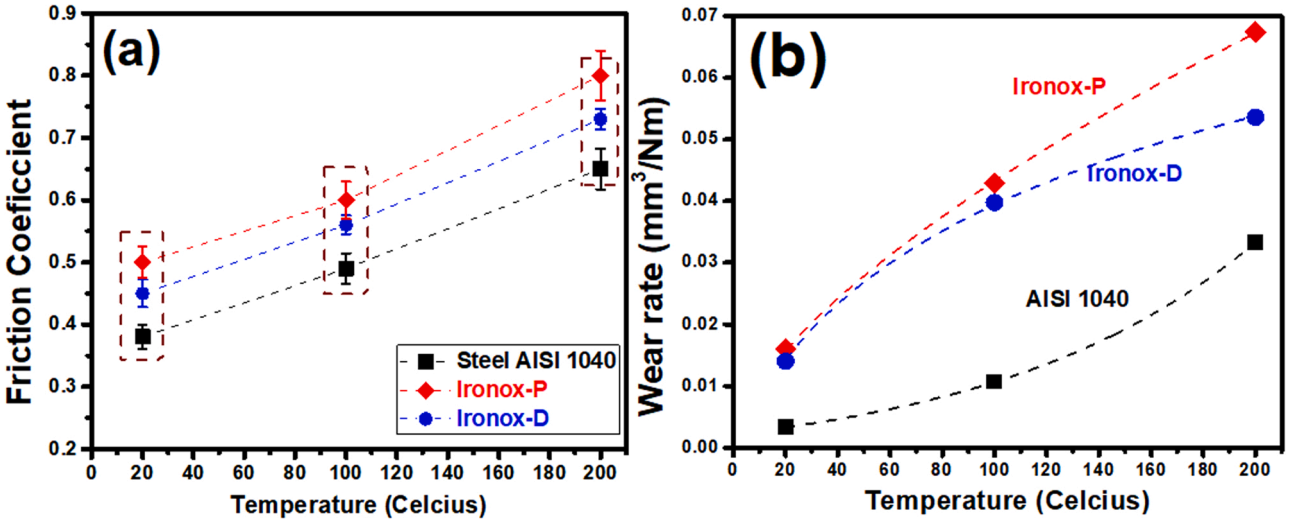

Fig. 6. Tribological Behavior for all samples as a function of the temperature for (a) friction coefficient and (b) wear rate.

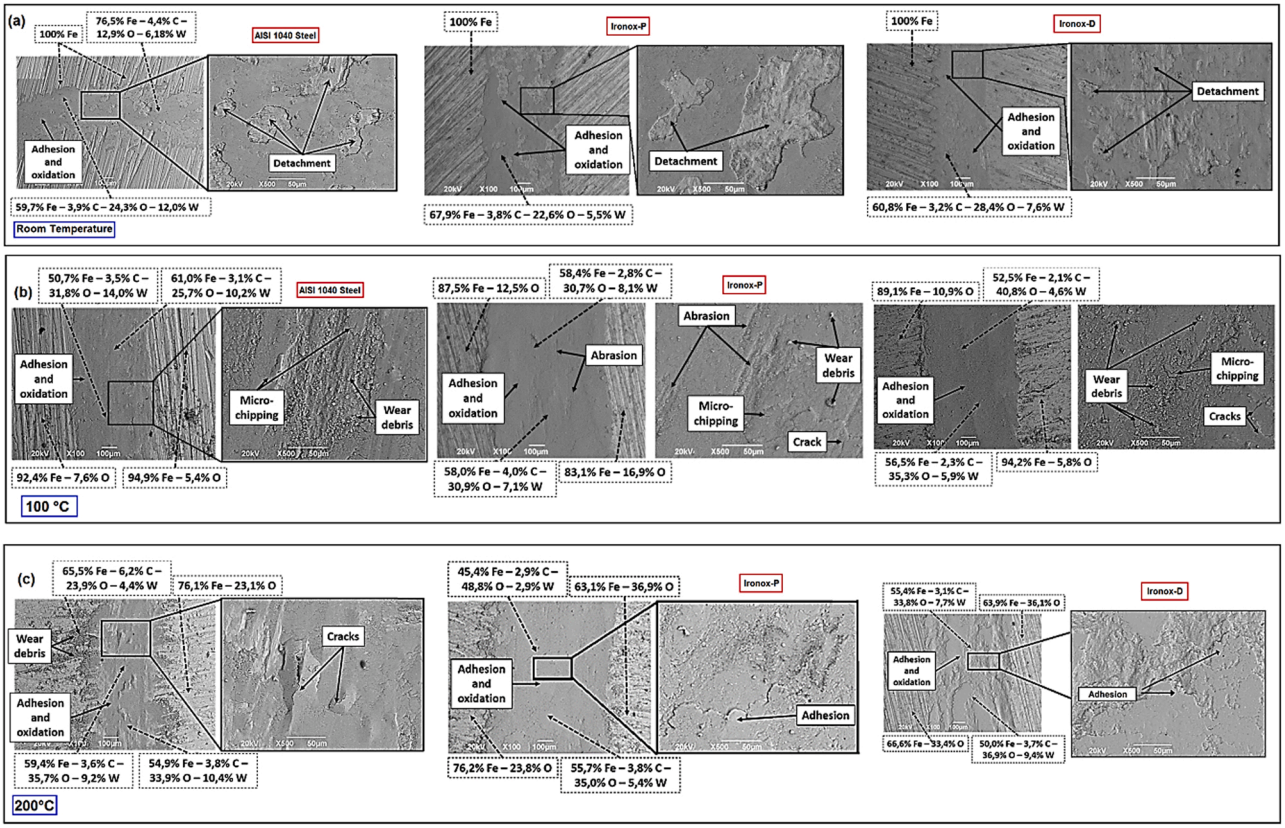

Fig. 7. SEM micrographs of the wear track for AISI 1040 steel, Ironox-P and Ironox-D as a function of temperature (a) room temperature, (b) 100 °C and (c) 200 °C.

evidenced as it was in the room condition. However, with the high temperature and the oxidation of material, there is a lot of material particulate on the surface. It can be attributed to the difficulty of smeared and the material when the counterpart passes over, which complicates the formation of a compact and homogeneous layer on top surface of the track. Indeed, come abrasion lines, produced by those free particles, can be observed as scars in the direction of sliding [5]. In this case, the width of the wear track is 400 μm, which is higher than in the case of room temperature, because of the ejection of particles from the contact. Fig. 7b shows some evidenced of micro-chipping, as micro-cracks, and shows the presence of some debris on the surface of the track, which, according to the chemical analysis, correspond to WC particles of the counterpart and oxidized particles of the sample. Moreover, the Fig. 7b shows the wear track of ironox-D at 100 °C. Adhesion and oxidation is observed, but there is no evidenced of detachment, layer formation or abrasion. Also, as in the case of ironox-P, a higher number of particles in the track is observed. The width of the wear track is 290 μm, which is higher than in the case of room temperature, but lowers than in the case of ironox-P at 100 °C. Wear particles observed correspond to WC debris of the counterpart and to oxidized material of the sample.

Finally, the Fig. 7c show SEM micrographs of the surface of AISI 1040

steel at 200 °C, including the wear track which width was 410 μm, where adhered oxidized material from the sample and WC from the counterpart was found according to EDS analysis. Then the wear debris was observed outside of the wear track, although detachment is not observed, crack formation. Fig. 7c shows the wear track of ironox-P at 200 °C. Adhesion as well oxidation is observed, but no detachment or layer formed in the track are evident. In this case, the width of the wear track is 540 μm, which is higher compared to test carried out at room temperature and 100 °C. Fig. 7c show the presence of some debris on the track, which according to the chemical analysis, correspond to WC particles of the counterpart and oxidized particles of the sample. Wear track of ironox-D at 200 °C show adhesion and oxidation and a width of 440 μm. Also, the Fig. 7c shows 3D profiles of wear surface of the samples at 200 °C. In average, track depth is deeper in wear surface of AISI 1040 steel (10.33 ± 0.5 μm) followed by ironox-D (11.81 ± 0.6 μm), while the least deep track is exhibited by the ironox-P (14.2 ± 0.71 μm).

Fig. 8 shows 3D profiles of wear surfaces of the samples at room temperature (Fig. 8a), samples with temperature of 100 °C (Fig. 8b), and samples with temperature of 200 °C (Fig. 8c), obtained by profilometry. The 3D profilometry results revealed the effect of compaction pressure on ironox-P and ironox-D compounds and further revealed the effect of working temperature on the wear test, thus clearly showing that the width of the wear track increases as the temperature increases, indicating how the mechanical properties are compromised by modifying the elastic modulus with the thermal effect thus increasing friction and wear.

*I*n average, abrasive wear and detachment is deeper in wear surface of ironox-P (7.26 μm ± 0.36) followed by ironox-D (4.11 μm ± 0.2), while the least deep track is exhibited by the AISI 1040 steel (2 μm ± 0.3), these values are presented in Fig. 9a obtained by profilometry in the room temperature. For the temperature of 100 °C in average, track depth is deeper in wear surface of AISI 1040 steel (4.15 μm ± 0.5) followed by ironox-D (5.86 ± 0.6), while the least deep track is exhibited by the ironox-P (10.4 μm ± 0.71), these values are presented in Fig. 9b obtained by profilometry. Moreover, for the temperature of 200 °C, in average, track deeper in wear surface of AISI 1040 steel (10.33 μm ± 0.5) followed by ironox-D (11.81 μm ± 0.6), while the least deep track is exhibited by the ironox-P (14.2 μm ± 0.71), these values are presented in Fig. 9c obtained by profilometry.

4. Discussions

4.1. Metallography images and hardness

As expected, AISI 1040 steel is harder than ironox compounds, because the higher hardness exhibited by the cementite than iron oxide, its laminar configuration, and the absence of porous in the steel. Higher hardness of ironox compacted at higher pressure is also evident. It is expected that higher compacting pressure produces lower porosity.

4.2. Roughness and porosity

Higher roughness and porosity of ironox compounds respect to AISI 1040 steel is attributed to the manufacturing process, which is compacting and sintering, which typically left porous in the material. This surface behavior was attributed to a higher external load applied during the compaction process, which produces a plastic deformation generated in them. In this way, micro-welds are produced between the

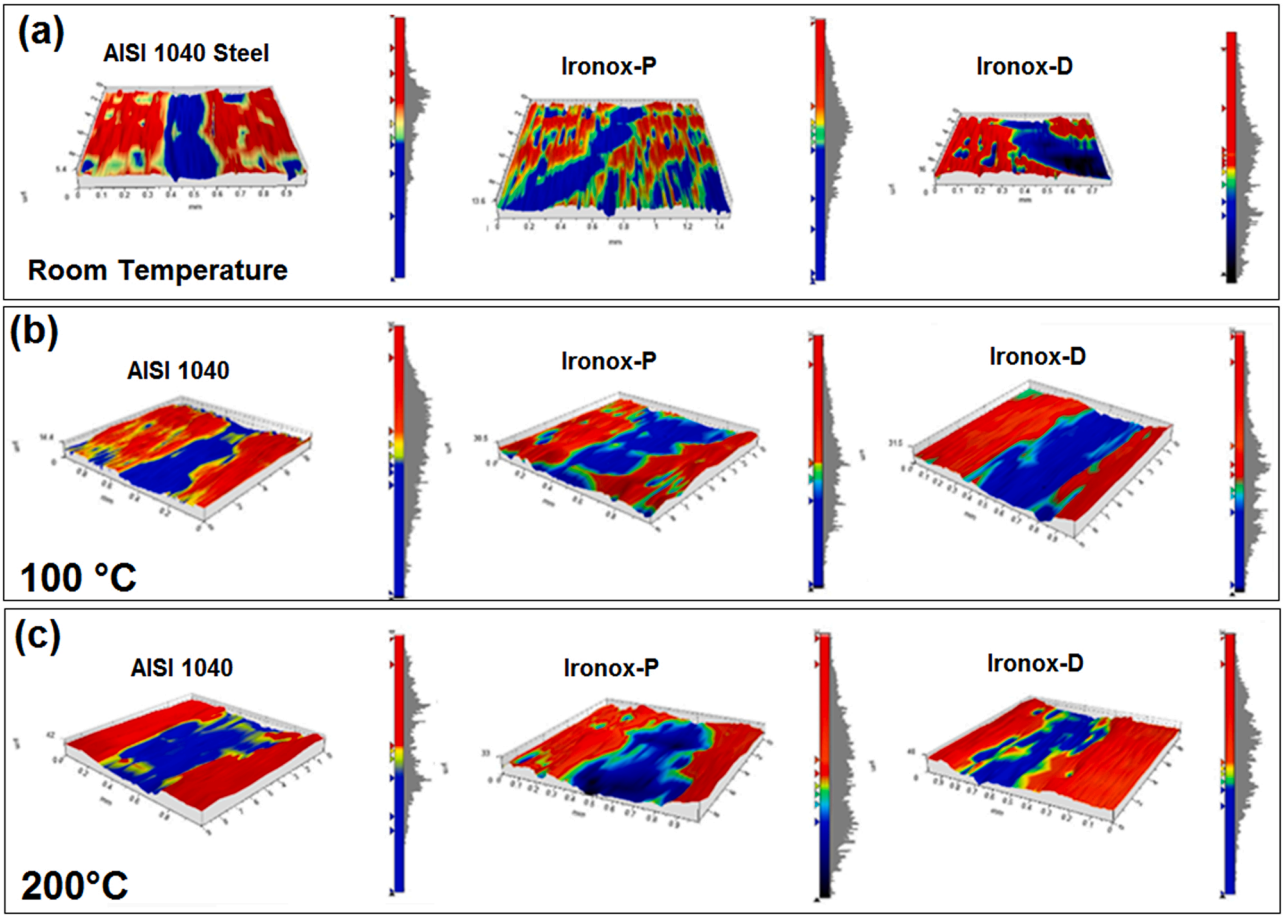

Fig. 8. 3D profiles of wear surfaces for AISI 1040 steel, ironox-P and ironox-D as a function of the temperature: (a) room temperature (b) 100 °C and (c) 200 °C.

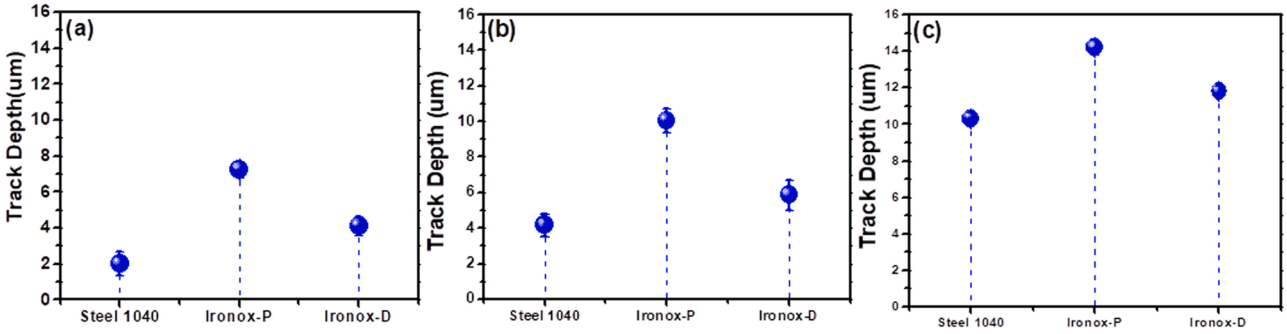

Fig. 9. Track Depth values for all samples: (a) room temperature, (b) 100 °C and (c) 200 °C.

particle, forming equiaxial particles, increasing the average particle size and causing a reduction of the pores [27,28].

4.3. Tribological analysis

4.3.1. Wear rate as a function of temperature

The wear rate of AISI 1040 steel with temperature are higher compared to what was observed for ironox-D or even ironox-P, when the trend seems to slow down as long as temperature increase.

This behavior is related to the phases and to the properties of the reinforcing second phase of each material. In the case of steel, cementite, which is the second reinforcing phase, is produced during the cooling of steel as the result of the eutectoid reaction. In this reaction, austenite transforms in ferrite plus cementite (Fe_3C), which is a microconstituent called pearlite. In annealed condition, at room temperature, an AISI 1040 steel is composed of 48.6 % of primary ferrite plus 51.4 % of pearlite, or 94.1 % of ferrite and 5.9 % of cementite. As can be seen, a steel is mainly composed of ferrite, which is a soft metallic phase which soften easily with temperature. Besides, when is heated, little quantities of cementite dissolved in the metallic phase. At 100 °C the quantity of pearlite diminishes up to 51.3 % and at 200 °C it diminishes up to 51.2 %. These two factors cause the mechanical properties of a steel to diminish with temperature increasing and was shown by Mahapatra et. al [6]. Among this research, a carbon steel with 0.16 % C exhibits a yield strength of 290 Mpa at 0 °C, while at 100 °C that value is of 260 Mpa and at 200 °C is of 230 Mpa. This decreasing in yield strength is due to the higher mobility of dislocations at high temperatures because of the weakening of the metallic chemical bond of ferrite.

In the case of ironox compounds, it is composed of 53 % of iron oxide (a mix of wüstite and magnetite) and 47 % of iron. Although iron oxide is not as hard as cementite or pearlite, it is a ceramic material with an ionic-covalent mix chemical bond. Iron is the soft phase, which soften with temperature. Therefore, because iron oxide does not dissolve in iron phase and because the softer phase is in a lower quantity than is steel, the increasing in wear rate of ironox compounds with temperature tends to slow down, while the wear rate in AISI 1040 steel tends to accelerate.

4.3.2. Friction coefficient as a function of temperature

As observed Fig. 10, shows the well-known influence of mechanical properties and surface conditions, as porosity in the friction coefficient. Indeed, higher friction coefficient values under tribological test were registered from ironox-P samples, which is mainly attributed to its roughness and lower hardness, compared to low values obtained from Ironox-D, and AISI 1040 steel samples.

The influence of the temperature on the tribological behavior show a general increase of friction coefficient values, which can be attributed to thermo-mechanical stress, high chemical interaction between counterparts, as well as high contact areas, produce all of them by high temperatures. These conditions favor oxidation, material transfer and adhesion phenomena. The contact accommodation was also modified by the temperature which allow reaching the steady stage. As oxidation is higher and generalized, a stable wear rate could be stablished on the surface, by the formation of wear debris and its ejection to sideway [29,30].

Moreover, about the running-in stage, a shorter stage that was observed in ironox-P at room temperature in comparison to AISI 1040 steel and ironox-D. It can be explained by a rapid and larger deformation

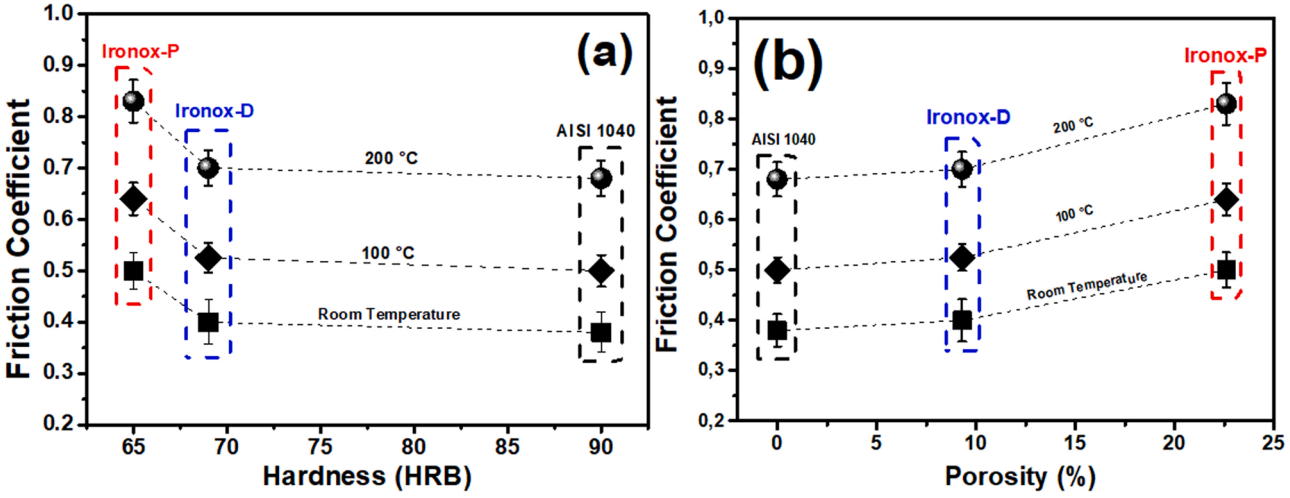

Fig. 10. Relationship between (a) friction coefficient versus hardness and (b) friction coefficient versus porosity for all samples as a function of the temperature used during the tribological test.

of the surface asperities of ironox-P suffered at higher temperature (Table 1). All curves from experiments under 200 °C show high wear rate as observed from Fig. 6. While for samples evaluated under 100 °C and room temperature the wear rate seems to be like a non-lubricated metals contact. At room temperature, for all samples, after the running-in stage, no steady state was reached at room temperature as expected. It could be explained by wear mechanisms observed: although oxidation occurs on the samples surface changing its surficial mechanism properties, the material is worn (Figs. 7–9).

4.3.3. *Tungsten content in the wear track as a function of samples hardness*

Besides abrasive wear, which is evident by 3D profiles (Fig. 8), adhesive and oxidative wear mechanism are also observed, as well as delamination or detachment of samples at room temperature. Even more, transfer from the counterpart occurs, according to the chemical EDS analysis. There is directly proportional relationship between the Tungsten (W) content in the wear track and the samples hardness (Fig. 11). This means that harder sample remove material easier from the counterpart than softer samples.

4.4. *Wear rate as a function of hardness*

Wear rate at room temperature as a function of materials hardness is observed in Fig. 12. As expected, the higher the hardness, the lower the wear rate of the samples. It means that AISI 1040 steel exhibits a lower wear rate than ironox compounds. In relation to the ironox compounds, the same behavior is observed: the ironox with higher hardness and lower porosity (ironox-D), has a lower wear rate compared to the ironox-P compound.

Furthermore, interesting changes are observed when the temperature during the tribological test increased with respect to the room temperature. This increase in wear rate is related to the elastic modulus of material and taking account that the crystalline structure of steel is composed of a molecular structure whose atoms of Fe, C and others are interacting through bonds. Therefore, when the temperature increases, the molecular vibration also increases, generating dilatation and compression mechanism that can affect the molecular electronic density of the structure and therefore affect the elastic modulus. In this sense, in materials such as steel, the elastic modulus is closely related to the wear rate. Thus, if the elastic modulus is modified by the effects of temperature, it can be observed that the wear resistance is affected by modifying the wear rate [31]. Subsequently, Fig. 12 shows the value of the friction coefficient for all samples as a function of the hardness used during the tribological test. These results showed that although the AISI 1040 steel

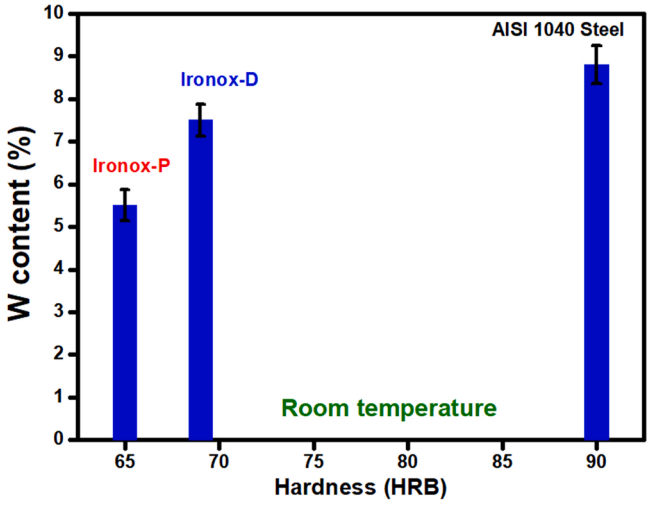

Fig. 11. Tungsten (W) content in the wear track at room temperature as a function of the hardness of the samples.

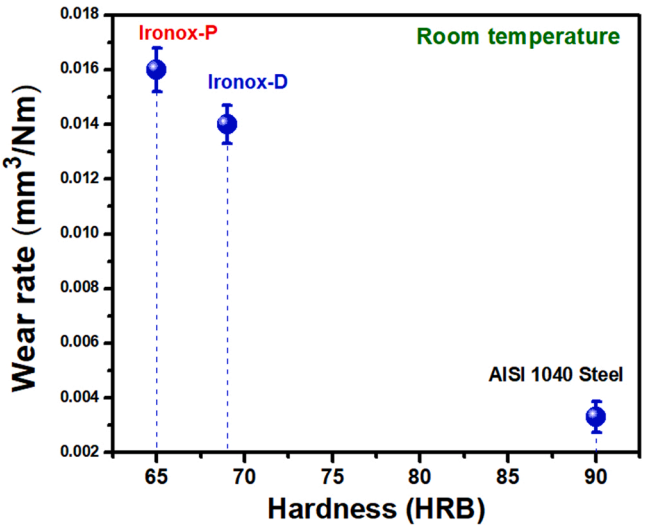

Fig. 12. Wear rate at room temperature as a function of hardness samples.

still shows a lower wear rate than the ironox composite, its wear rate tends to grow exponentially as the temperature increases. Furthermore, the wear rate of ironox as a function of temperature increases as a function of second order. Therefore, the wear rate of ironox tends to decrease as the temperature increases, while the wear rate of steel accelerates.

Also, adhesive wear increased with the temperature. Softening caused by the temperature increase leads to the adhesion because the material can suffer higher plastic deformation of the asperities, which in turn leads to higher wear rate and wider wear track as observed in Fig. 13, where oxidized material is obtained because of the temperature increments. At 200 °C, although micro-chipping is not so obvious on the surface of AISI 1040 steel surface, some cracks are visible. 3D profile analysis corroborates the higher wear rate at this temperature, which, as was indicated at 100 °C, is caused by the softening of ferrite, which is the soft phase. However, the highest oxidation of the surface tends to diminish the microchipping (Fig. 7). The rougher surfaces exhibited by the ironox compounds (Fig. 7) indicates that these materials are susceptible to adhesive phenomena than to oxidation, in the case of steel. Some debris are also observed, in the case of ironox- P, indicating that microchipping could also occurred [32].

5. Conclusions

The tribological behavior of an innovative material called ironox was

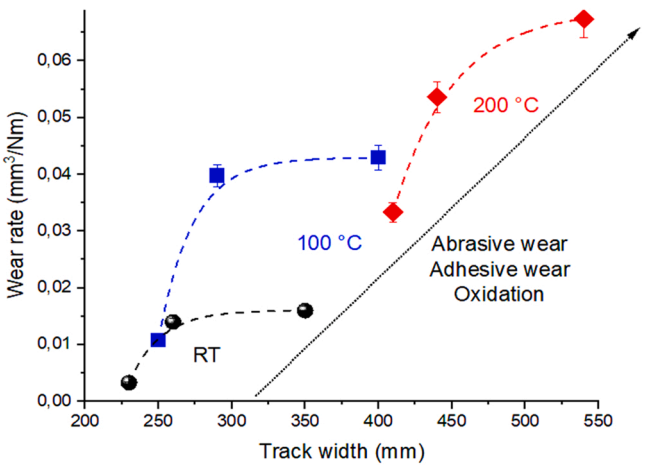

Fig. 13. Relationship between wear rate of the sample and the track width.

achieved, finding the next main results:

- In the tribological behavior was observed that the increasing in wear rate of ironox compounds with high temperature tends to slow down, while the wear rate in AISI 1040 steel tends to accelerate. However, the AISI 1040 steel is harder and more resistance to wear than ironox compounds, as iron oxide dissolve in iron phase and the softer phase is a high quantity than in AISI 1040 steel.
- The increasing in wear rate of ironox compounds with temperature tends to slow down, while the wear rate in AISI 1040 steel tends to accelerate. This last one is harder and more resistant to wear than ironox compounds, as iron oxide dissolves in iron phase and the softer phase is in a lower quantity than in steel.
- Wear mechanisms found in all the sample at all temperatures were abrasion, adhesion and oxidation. However, beside those phenomena, at room temperature detachment is found, while at high temperature cracking and micro-chipping were observed.
- Denser ironox exhibited better tribological behavior than porous ironox, exhibiting lower friction coefficient as well as lower wear rate.

Declaration of Competing Interest

The authors declare that they have no known competing financial interests or personal relationships that could have appeared to influence the work reported in this paper.

Data availability

Data will be made available on request.

Acknowledgments

Authors thank to Escuela Colombiana de Ingeniería Julio Garavito and Universidad del Valle for financing this Project, as well as Gerdau-Diaco for proving the material of stufy.

This research was supported by the Tribology, Polymers, Powder Metallurgy and Solid Waste Transformations research group of the Universidad del Valle; Recubrimientos Duros y Aplicaciones Industriales (RDAI) research laboratory of the Universidad del Valle.

References

[1] Eissa M, Ahmed A, El-Fawkhry M. Conversion of mill scale waste into valuable products via carbothermic reduction. J Met 2015;2015:1–9. https://doi.org/10.1155/2015/926028.
[2] Sustainable consumption and production – United Nations Sustainable Development, (n.d.). ⟨https://www.un.org/sustainabledevelopment/sustainable-consumption-production/⟩ (accessed November 15, 2021).
[3] Política Nacional de Producción y Consumo Sostenible - Red de Desarrollo Sostenible de Colombia, (n.d.). ⟨https://www.rds.org.co/es/recursos/politica-nacional-de-produccion-y-consumo-sostenible⟩ (accessed November 16, 2021).
[4] Tirado González JG, Reyes Segura BT, Esguerra-Arce J, Bermúdez Castañeda A, Aguilar Y, Esguerra-Arce A. An innovative magnetic oxide dispersion-strengthened iron compound obtained from an industrial byproduct, with a view to circular economy. J Clean Prod 2020;268:122362. https://doi.org/10.1016/j.jclepro.2020.122362.
[5] Howson TE, Mervyn DA, Tien JK. Creep and stress rupture of a mechanically alloyed oxide dispersion and precipitation strengthened nickel-base superalloy. Metall Trans A 1980;11:1609–16. https://doi.org/10.1007/BF02654525.
[6] Zhou Y, Gao Y, Wei S, Pan K, Hu Y. Preparation and characterization of Mo/Al2O3 composites. Int J Refract Met Hard Mater 2016;54:186–95. https://doi.org/10.1016/j.ijrmhm.2015.07.033.
[7] Tu S. Emering to structural integrity technology for high-temperature applications. Front Mech Eng 2007:375–87.
[8] Sista KS, Dwarapudi S, Nerune VP. Direct reduction recycling of mill scale through iron powder synthesis. ISIJ Int 2019;59:787–94. https://doi.org/10.2355/isijinternational.ISIJINT-2018-628.
[9] Askeland DR. The science and engineering of materials. Sci Eng Mater 1996. https://doi.org/10.1007/978-1-4613-0443-2.
[10] Elhadi A, Bouchoucha A, Jomaa W, Zedan Y, Schmitt T, Bocher P. Study of surface wear and damage induced by dry sliding of tempered AISI 4140 steel against hardened AISI 1055 steel. Tribol Ind 2017;38:475–85.
[11] Panin V, Kolubaev A, Tarasov S, Popov V. Subsurface layer formation during sliding friction. Wear 2001;249:860–7. https://doi.org/10.1016/S0043-1648(01)00819-5.
[12] Fleming JR, Suh NP. Mechanics of crack propagation in delamination wear. Wear 1977;44:39–56. https://doi.org/10.1016/0043-1648(77)90083-7.
[13] Study of surface wear and damage induced by dry sliding of tempered, (n.d.).
[14] Zambrano OA, Gómez JA, Coronado JJ, Rodríguez SA. The sliding wear behaviour of steels with the same hardness. Wear 2019;418–419:201–7. https://doi.org/10.1016/j.wear.2018.12.002.
[15] Surface film formation and metallic wear, Wear. 1 (1957) 163. ⟨https://doi.org/10.1016/0043–1648(57)90019–4⟩.
[16] Bahrami A, Soltani N, Pech-Canul MI, Gutiérrez CA. Development of metal-matrix composites from industrial/agricultural waste materials and their derivatives. Crit Rev Environ Sci Technol 2016;46:143–208. https://doi.org/10.1080/10643389.2015.1077067.
[17] Deaquino-Lara R, Soltani N, Bahrami A, Gutiérrez-Castañeda E, García-Sánchez E, Hernandez-Rodríguez MAL. Tribological characterization of Al7075-graphite composites fabricated by mechanical alloying and hot extrusion. Mater Des 2015;67:224–31. https://doi.org/10.1016/j.matdes.2014.11.045.
[18] Bahrami A, Pech-Canul MI, Gutierrez CA, Soltani N. Effect of rice-husk ash on properties of laminated and functionally graded Al/SiC composites by one-step pressureless infiltration. J Alloy Compd 2015;644:256–66. https://doi.org/10.1016/j.jallcom.2015.04.194.
[19] Soltani N, Jafari Nodooshan HR, Bahrami A, Pech-Canul MI, Liu W, Wu G. Effect of hot extrusion on wear properties of Al–15wt% Mg2Si in situ metal matrix composites. Mater Des 2014;53:774–81. https://doi.org/10.1016/j.matdes.2013.07.084.
[20] Bahrami A, Soltani N, Pech-Canul M. Effect of sintering temperature on tribological behavior of Ce-TZP/Al 2 O 3 -aluminum nanocomposite. J Compos Mater 2015;49:3507–14. https://doi.org/10.1177/0021998314567010.
[21] Agrawal R, Mukhopadhyay A. Optimization of wear performance and COF of AISI 1040 steel using grey relational analysis. Mater Today Proc 2022. https://doi.org/10.1016/j.matpr.2022.03.665.
[22] Li X, Sosa M, Olofsson U. A pin-on-disc study of the tribology characteristics of sintered versus standard steel gear materials. Wear 2015;340–341:31–40. https://doi.org/10.1016/j.wear.2015.01.032.
[23] Conshohocken W. Standard test method for wear testing with a pin-on-disk apparatus 1. Wear V 2007:1–5.
[24] King PC, Reynoldson RW, Brownrigg A, Long JM. Pin on disc wear investigation of nitrocarburised H13 tool steel. Surf Eng 2005;21:99–106. https://doi.org/10.1179/174329405×40911.
[25] Federici M, Straffelini G, Gialanella S. Pin-on-disc testing of low-metallic friction material sliding against HVOF coated cast iron: modelling of the contact temperature evolution. Tribol Lett 2017;65:121. https://doi.org/10.1007/s11249-017-0904-y.
[26] Munagala VNV, Chromik RR. The role of metal powder properties on the tribology of cold sprayed Ti6Al4V-TiC metal matrix composites. Surf Coat Technol 2021;411:126974. https://doi.org/10.1016/j.surfcoat.2021.126974.
[27] Poquillon D, Baco-Carles V, Tailhades P, Andrieu E. Cold compaction of iron powders - relations between powder morphology and mechanical properties: Part II. Bending tests: results and analysis. Powder Technol 2002;126:75–84. https://doi.org/10.1016/S0032-5910(02)00035-9.
[28] Korim NS, Hu L. Study the densification behavior and cold compaction mechanisms of solid particles-based powder and spongy particles-based powder using a multi-particle finite element method. Mater Res Express 2020;7. https://doi.org/10.1088/2053-1591/ab8cf6.
[29] Vergne C, Boher C, Levaillant C, Gras R. Analysis of the friction and wear behavior of hot work tool scale: application to the hot rolling process. Wear 2001;250:322–33. https://doi.org/10.1016/S0043-1648(01)00598-1.
[30] Liang C, Wang C, Zhang K, Tan H, Liang M, Xie Y, et al. The study of mechanical and tribology properties at room- and high-temperature in a (NiCoFe)86.5(AlTi)12(WMoV)1.5 high-entropy alloy. J Alloy Compd 2022;911:165082. https://doi.org/10.1016/j.jallcom.2022.165082.
[31] Serebriakov I, Puchi-Cabrera ES, Dubar L, Moreau P, Meresse D, Barbera-Sosa JGLa. Friction analysis during deformation of steels under hot-working conditions. Tribol Int 2021;158:106928. https://doi.org/10.1016/j.triboint.2021.106928.
[32] Lancaster JK. The influence of temperature on metallic wear. Proc Phys Soc Sect B 1957;70:112–8. https://doi.org/10.1088/0370-1301/70/1/316.